

Utilization of Ambient Gas as a Propellant for Low Earth Orbit
Electric Propulsion

by

Buford Ray Conley

Submitted to the

Department of Aeronautics and Astronautics
in Partial Fulfillment of the Requirements for the
Degree of

MASTER OF SCIENCE

in Aeronautics and Astronautics

at the

Massachusetts Institute of Technology

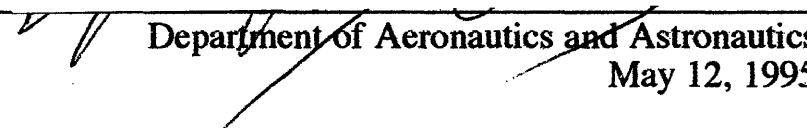
May 1995

© 1995 Buford Ray Conley

All rights reserved

The author hereby grants to MIT permission to reproduce and to distribute publicly paper
and electronic copies of this thesis document in whole or in part.

Signature of Author


Department of Aeronautics and Astronautics
May 12, 1995

Certified by


Professor Jack L. Kerrebrock
Thesis Supervisor

Accepted by


Professor Harold Y. Wachman

Chairman, Departmental Graduate Committee

MASSACHUSETTS INSTITUTE
OF TECHNOLOGY

JUL 07 1995

LIBRARIES

Abstract

Atmospheric drag is a significant driver in systems design for Low Earth Orbit (LEO) satellites. Drag due to ambient LEO gas limits lifetime and sometimes necessitates heavy propulsion systems. This research investigates utilizing the atmospheric gas as a propellant for an ion engine. This new ion propulsion system could be used for station keeping for balancing the drag force or for providing attitude control.

It is found that this concept is only applicable at an altitude of about 200 Km due to trades between propellant and power requirements. An innovative ion thruster 5 meters in length and 15 meters in radius can negate the drag force on a satellite of one square meter area using 2900 Watts. However, the thruster's large size and potential problems with stowage and deployment will require further analysis to determine its utility. The advantages of low subsystem weight and extended spacecraft lifetime are significant compared to the extra power requirements. As a step in the analysis of this concept, Child's law for space charge limited current is derived for the case of a non-zero initial velocity. The space charge limitation is also derived in a cylindrical geometry in the presence of an axial magnetic field perpendicular to a radial electric field.

TABLE OF CONTENTS

1. TRENDS IN COMMUNICATIONS SATELLITES.....	5
1.1 LOW ORBITS	5
1.2 SATELLITE DRAG AND PROPULSION	5
2. LEO ION THRUSTER CONCEPT	6
2.1 DESIGN OVERVIEW	6
2.2 USE AMBIENT GAS FOR PROPELLANT	6
2.3 ESTIMATE OF POWER REQUIREMENTS	6
2.4 ALTITUDE CONSTRAINTS FOR CONCEPT.....	10
2.5 DESIGN REQUIREMENTS.....	10
2.6 DESIGN PARAMETERS	10
2.6.1 <i>Electric Fields</i>	10
2.6.2 <i>The Magnetic Field</i>	11
2.6.3 <i>Ionization Chamber Length</i>	11
2.6.4 <i>Thruster Radius</i>	11
3. DESIGN ANALYSIS	11
3.1 THRUST LEVEL REQUIREMENTS.....	11
3.2 IONIZATION CAVITY DESIGN	12
3.2.1 <i>General Considerations</i>	12
3.2.2 <i>Magnetic Field Configuration</i>	12
3.2.3 <i>Larmor Radius and Sizing</i>	12
3.2.4 <i>Ionization Mechanics</i>	13
3.2.4.1 <i>The Collision Probability</i>	13
3.2.4.2 <i>Free-Paths and Transit Times of the Surviving Neutrals</i>	14
3.2.4.3 <i>The Mean Free Path and Probabilities</i>	15
3.2.4.4 <i>The Ionization Rate of a Constant Speed Electron Beam Moving Through a Gas of Neutrals</i>	16
3.2.4.5 <i>Ionization Cross Section</i>	16
3.2.5 <i>Space Charge Limitations in the Presence of a Magnetic Field</i>	17
3.2.6 <i>Ion Mass Flux</i>	18
3.2.6.1 <i>Ionization Frequency in the Magnetic Field</i>	18
3.2.6.2 <i>Ionization Fraction and Mass Flux</i>	19
3.3 CONFIGURATION OF THE ACCELERATOR.....	21
3.3.1 <i>Space Charge Limited Current</i>	21
3.3.1.1 <i>Poisson's Equation</i>	22
3.3.1.2 <i>The Electric Field of an Ion Current Entering the Grid</i>	23
3.3.1.3 <i>Integration of Poisson's Equation</i>	23
3.3.1.4 <i>Practical LEO Space Charge Limited Current Value</i>	25
3.4 DESIGN OPTIMIZATION	25
3.4.1 <i>Ionizer Power</i>	26
3.4.2 <i>Jet Power</i>	26
3.4.3 <i>Total Power</i>	26
3.4.4 <i>Thrust Requirements</i>	26
3.4.5 <i>Optimization of Physical Dimensions for Minimum Power</i>	27
3.4.6 <i>Example Values</i>	28
4. CONCLUSIONS AND RECOMMENDATIONS.....	28
4.1 APPLICABILITY OF ION PROPULSION TO LEO SATELLITES.....	28
4.2 SUGGESTIONS FOR FURTHER ANALYSIS.....	29
4.3 SUGGESTIONS FOR DESIGN IMPROVEMENTS.....	29
5. APPENDIX.....	30

FIGURES

FIGURE 2-1 LEO ION THRUSTER CONCEPT.....	7
FIGURE 2-2 THRUSTER CONFIGURATION.....	8
FIGURE 2-3 PROPELLANT MASS VERSUS ALTITUDE.....	9
FIGURE 2-4 POWER VERSUS ALTITUDE.....	9
FIGURE 3-1 COLLISION CYLINDER.....	16
FIGURE 3-2 IONIZATION CROSS SECTION VERSUS ELECTRON ENERGY.....	17
FIGURE 3-3 ION RATE VERSUS RADIUS AND MAGNETIC FIELD.....	19
FIGURE 3-4 ION FRACTION VERSUS LENGTH AND MAGNETIC FIELD.....	20
FIGURE 3-5 FLUX VERSUS GEOMETRY.....	21
FIGURE 3-6 POWER VERSUS GEOMETRY.....	27
FIGURE 3-7 POWER VERSUS GEOMETRY (LOCAL VIEW).....	28

1. Trends in Communications Satellites

1.1 Low Orbits

Increasing demand for mobile communications systems has prompted many to consider the utilization of Low Earth Orbits (LEO) for constellations of satellites. The LEO constellations allow for significant reductions in spacecraft and user transmission power requirements. The lower power requirement is due to the small distance between the satellite and the ground user, which is usually a few hundred kilometers. As a comparison, a satellite at a geosynchronous orbit (GEO) is over 35786 Km from a ground user. Path losses increase with the square of the distance, resulting in a significant difference in transmitted power between LEO and GEO configurations.

At lower altitudes, satellite coverage is diminished, requiring more satellites. This increased recurring cost can be offset by lower unit costs and reduced launch costs. The unit costs are partially driven by the bus power, which is driven by transmitter power. As a result, LEO satellites tend to be much cheaper than GEO satellites. For example, a commercial geosynchronous satellite can cost well over \$250M while an Orbital Sciences Orb Com (LEO) is about \$1.5M. Furthermore, system mass is driven by power requirements. Solar panels, batteries, and associated support structures decrease as power is decreased. The combination of lighter satellites and lower altitudes result in significant savings in launch vehicle costs. For example, an Atlas rocket placing a single satellite into GEO transfer orbit costs about \$100M. An additional propulsion system is needed to raise the orbit from GEO transfer to GEO synchronous orbit, adding a few million dollars more. These costs can be compared to a LEO satellite launched from a Pegasus costing about \$10M. Note further, that in many cases multiple satellites can be carried in one Pegasus launch, decreasing the launch cost per satellite further.

After reviewing these system constraints and costs, LEO based systems look very attractive. However, there is a catch. In LEO there is still some atmosphere. This low density gas causes drag and surface degradation. The drag perturbs the orbit, requiring either counteractive propulsion or system margin for orbit variations and decay. The oxygen attacks the solar panels and other exposed surfaces causing damage and deterioration. These combined factors result in LEO satellite designs with lifetimes on the order of 2 years. This contrasts sharply with GEO satellites which have life times of almost 15 years (HS-601). As a result, the order of magnitude price differences per unit between LEO and GEO is almost negated by the excessive recurring cost of replacing LEO satellites so often. As a result, the GEO and LEO systems cost are nearly comparable. However, with the advent of hand-held personal communicators, the LEO configuration presents significant technological advantages. These include reduced power requirements at both the transponder and receiver, and a reduction in signal delay time.

1.2 Satellite Drag and Propulsion

Extending the operational lifetime of LEO satellites would make their system designs even more cost competitive with GEO configurations. The LEO spacecraft lifetime tends to be limited by the propulsion subsystem. Necessarily, when the satellite runs out of fuel, its orbit will decay and the spacecraft will become useless. Using more fuel increases system mass and adds to the launch costs. As a result, there is a strong motivation for increasing the performance of the propulsion subsystem. Increasing the specific impulse (Isp) is one way of doing this.

If the ambient gas is utilized as a propellant, there is no longer a launch vehicle weight penalty for fuel requirements. In fact, a propulsion system which draws upon the environment for the fuel has an effectively infinite specific impulse. The new constraints for such a device are the power requirements and thruster sizing. These constraints will now be considered for the LEO environment.

2. LEO Ion Thruster Concept

A propulsion system is necessary to enable satellites to operate in very low orbits. The cumulative drag effects on satellites in low orbits cause altitude loss and eventual atmospheric re-entry. Propulsion systems are necessary to negate the drag and prevent the early demise of the spacecraft's mission.

Since there is enough ambient gas to cause drag on a spacecraft, there should be enough to use as a propellant for an ion engine which could provide a balancing thrust. More specifically, a design which ionizes a stream of ambient gas and accelerates the ions should be able to provide a drag balancing thrust at a reasonable power.

2.1 Design Overview

The thruster consists of two stages. In the first stage the high velocity, ambient gas is ionized by collisions with energetic electrons. In the second stage, this mixture of neutrals and ions flow into an electrostatic field. The neutrals exit the thruster without incident, but the ions are accelerated by the field. The accelerated ions are unimpeded by the neutrals because of the low density, collisionless flow. This arrangement is conceptually depicted in Figure 2-1 and Figure 2-2.

The ambient gas is allowed to pass freely through the center of the thruster without being slowed. The ionizer consists of a swarm of electrons contained by a solenoid generated magnetic field. The radius of the ionization chamber is a function of the electron energy and magnetic field strength. The length of the chamber drives the fraction of neutrals which are ionized.

The accelerator consists of two parallel, fine wire meshes. The mesh serves only to support a charge to create an accelerating electric field. The spacing of the mesh is driven by space charge limitations on the current density of ions.

2.2 Use Ambient Gas for Propellant

The thruster uses ambient gas in the LEO environment as a propellant. The thrust is proportional to the mass flux of propellant. Similarly, the drag is directly proportional to the mass flux of the gas impinging on the spacecraft surface. Assuming the ion engine has a specific impulse of 1600 seconds, the propellant requirements for a 5 year mission can be determined as a function of orbital altitude, as shown in Figure 2-3.

The utility of an ambient gas thruster is limited to altitudes around 200 Km or lower. At higher altitudes, the propellant requirements are so small that it would be better to simply carry aboard the required propellant and use a traditional thruster technology.

2.3 Estimate of Power Requirements

At first order, the power requirement of an electric propulsion system is the product of the kinetic energy of the beam and the propulsive efficiency. Since the thrust equals the drag for our purposes, it is instructive to consider the power consumed by an electric thruster at various altitudes. The power requirement for an engine operating with an Isp of 1600 seconds is depicted in Figure 2-4.

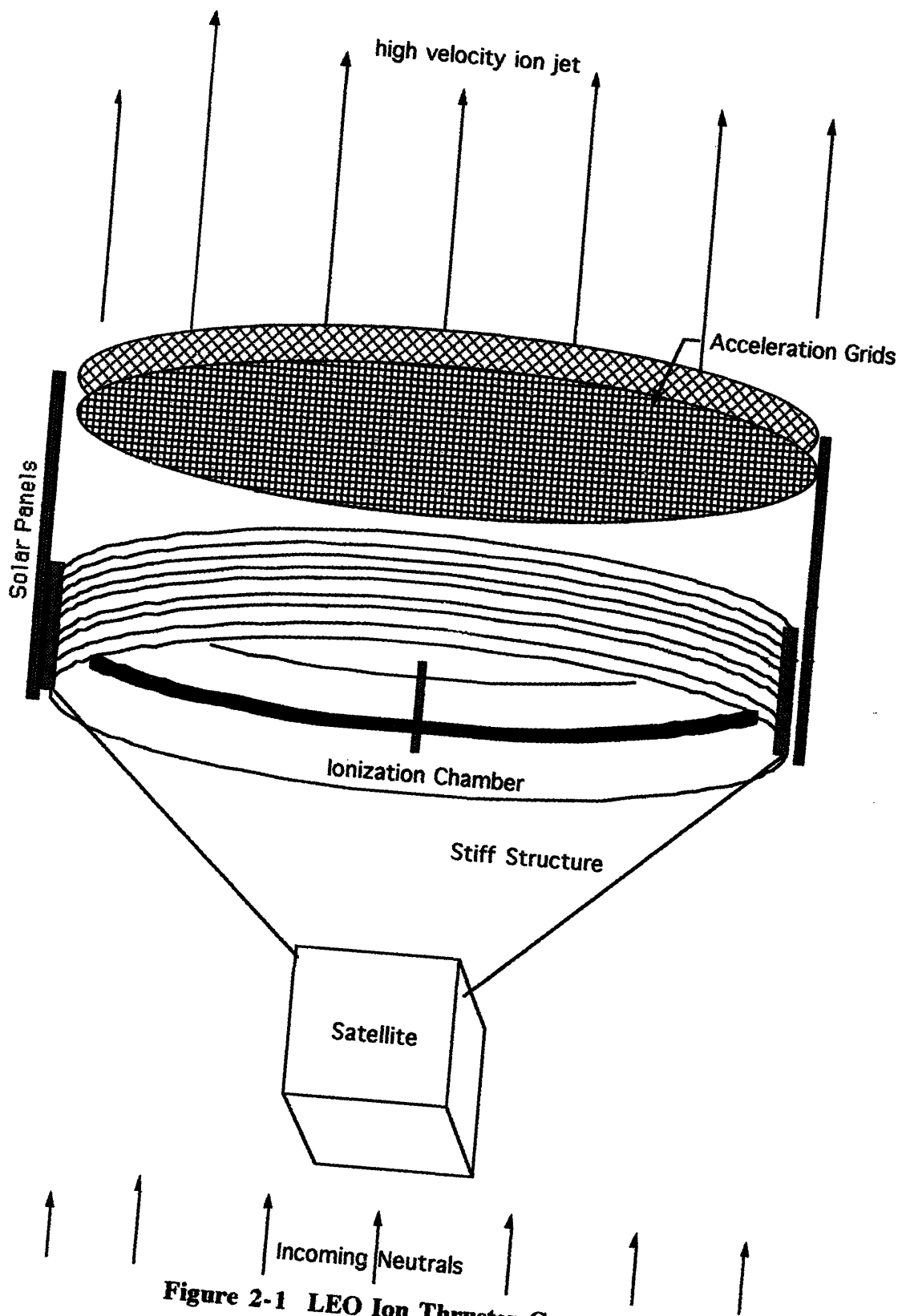


Figure 2-1 LEO Ion Thruster Concept

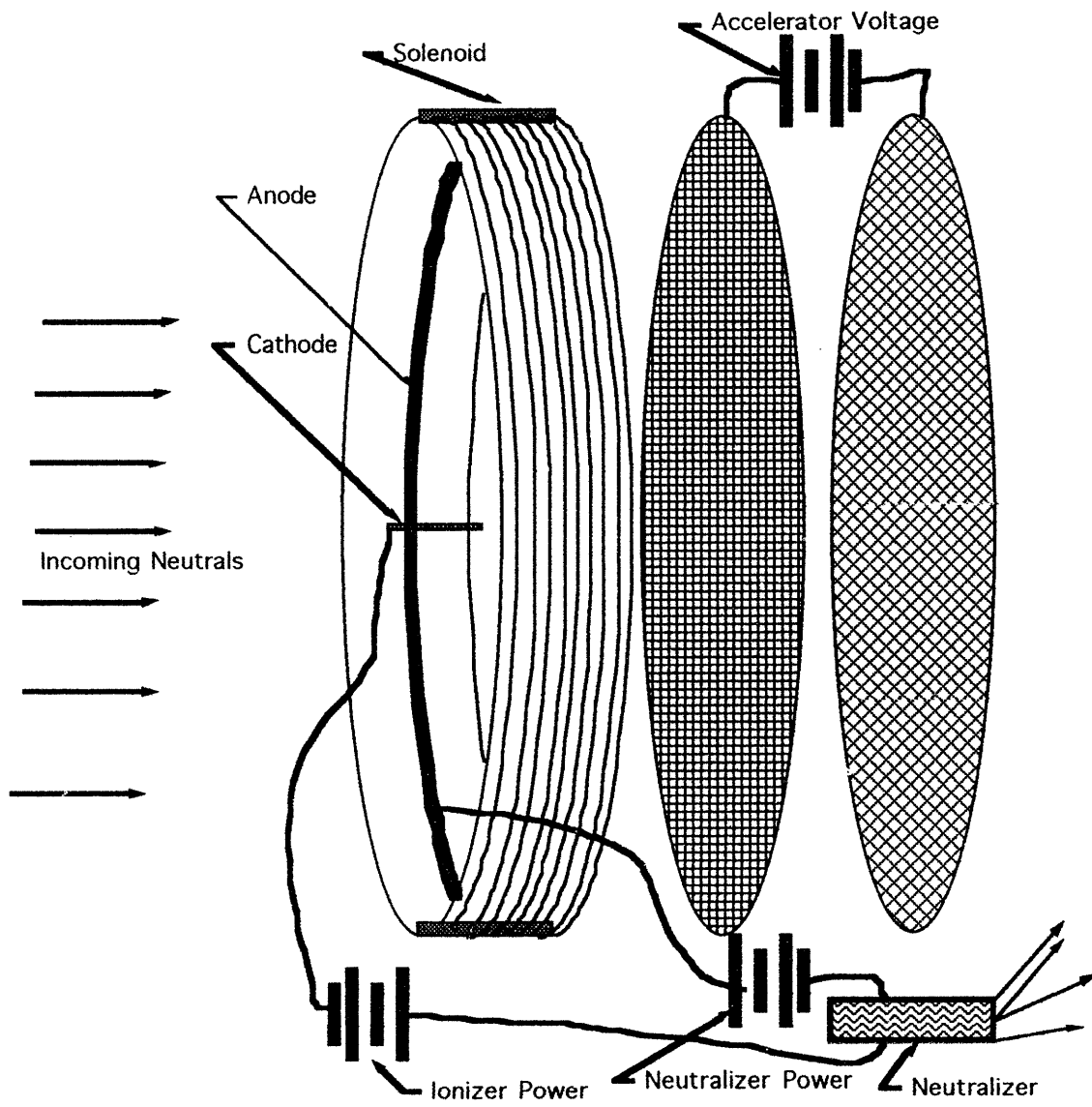


Figure 2-2 Thruster Configuration

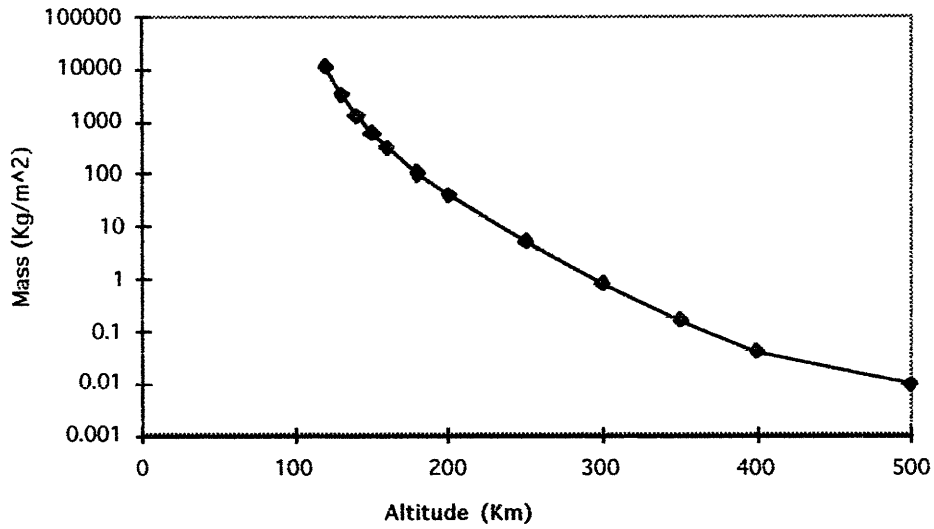


Figure 2-3 Propellant Mass Versus Altitude

Power Requirements at 1600 sec

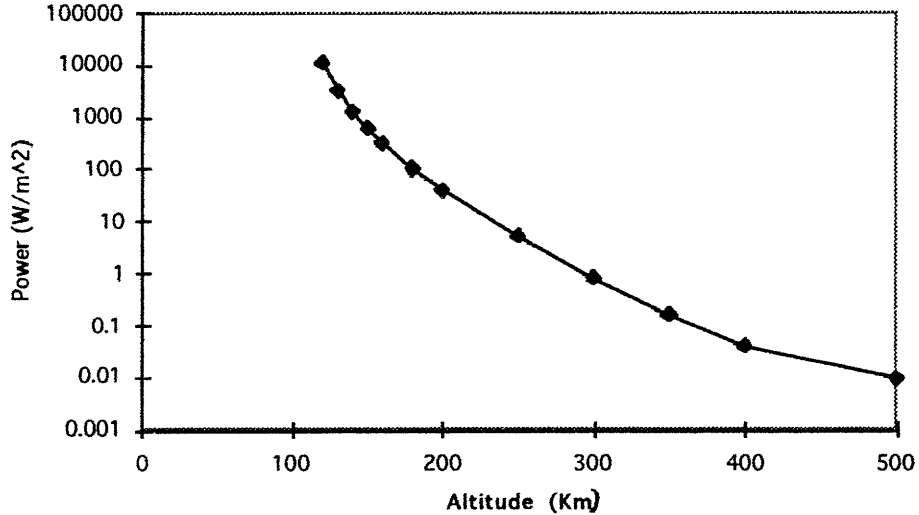


Figure 2-4 Power Versus Altitude

Current solar cell technology is capable of producing almost 210 Watts/m²¹. Assuming the solar cells also contribute to the drag, the proposed concept can only operate around an altitude of 200 Km or higher. At lower altitudes, the power requirement to negate drag is greater than the solar panel (which is causing drag) is capable of providing.

¹ Agrawal, Brij N. *Design of Geosynchronous Spacecraft* Prentice Hall. 1986

2.4 Altitude Constraints for Concept

The propellant requirements combined with the power demands indicate that the concept is limited to use at an altitude of about 200 Km. At higher altitudes, the propellant needs are low and do not justify the use of ambient gas. At lower altitudes, the power requirements are greater than existing solar cell technology can provide.

2.5 Design Requirements

The design of the LEO ion thruster should satisfy the following requirements:

1. The thruster must operate longer than the lifetime limiting subsystem.
2. The thruster must negate the effects of atmospheric drag.
3. The thruster must be small or deployable to allow stowage in faring.
4. The thruster must not interfere with the communications mission.

Since the objective of using the ion thruster is to extend the operational lifetime of the spacecraft, the thruster's longevity should not be the limiting factor. Other subsystems will degrade and limit the spacecraft lifetime or obsolescence will determine the maximum mission time. For example, atomic oxygen is very reactive, and will cause solar panel degradation. If the solar panels degrade beyond their power requirements, they will be the life limiting factor.

As the ions are accelerated, some collide with the thruster's accelerator grids. Impingement of high velocity ions causes sputtering. Sputtering is when an ion strikes a surface with such force that the atoms of the surface are dislodged. In existing ion propulsion systems the operational lifetime of the accelerator grids is 15 years, although they are capable of lasting nearly 30 years with degraded performance. This long lifetime is achieved by careful design of the accelerating electric fields to focus the ions in such a way that sputtering is limited. Also, the grids are made of materials resistive to sputtering.

Since the thruster must negate the drag on a spacecraft, the system design of the spacecraft will drive the size and power requirements of the thruster. Once the optimum thruster size is selected, the mechanical design must allow for efficient stowage and reliable deployment. The thruster is physically composed of a wire solenoid and two wire mesh grids. The grids could be stowed by placing them together and folding the mesh like a napkin. Upon deployment, springs could unfold the napkin into its operational configuration. The solenoid is ribbon-like circular loop of wire. This ribbon could be severed and coiled for stowage. When deployed, the ribbon can be uncoiled and re-connected at the severed point.

The magnetic field of the ionization cavity will allow variation of electron energy and gyro radius. This will determine the electromagnetic spectrum of noise generated by the thruster. The properties of this noise must be compared to the communications mission of the spacecraft to prevent any interference.

2.6 Design Parameters

2.6.1 Electric Fields

The electric field, between the anode and cathode of the ionizer, energizes electrons. As the electric field strength is increased, the electrons gain energy. However, at the higher potentials, more power will be drawn by the ionizer. The result is a trade between higher ionization rates and higher power.

The electric field between the accelerator grids determines the velocity boost imparted to the ions. The higher the electric field, the greater the thrust and the greater the ion flux which can be drawn due to space charge limitations. However, the ion beam must be neutralized. Since electrons from the neutralizer must be raised to the ions' potential, increasing electric field strength increases the neutralizer's power requirements. Again there is a trade between high thrust and high power requirements.

2.6.2 The Magnetic Field

The magnetic field in the ionizer determines the path of the energetic electrons. As the magnetic field strength is increased, the gyro radius of the electrons decreases, decreasing the size of the ionizer. When the inlet area of the thruster is decreased, the total neutral flux into the ionizer is decreased. The magnetic field must be optimized between achieving a high electron density, and producing a large ion flux.

2.6.3 Ionization Chamber Length

The ionization chamber length determines how long a neutral will travel through the electron swarm. Longer lengths increase the residence time of neutrals and their probability of being ionized. The longer length can also increase the mass of the thruster and its practicality for stowage.

2.6.4 Thruster Radius

The thruster radius determines the total flux of neutrals into the ionization chamber. A high flux of neutrals corresponds to a high ionizer power. However, the accelerator will have a lower velocity boost for a higher mass flux at a given thrust. As a result, the neutralizer power decreases with increasing radius. The thruster radius must be optimized to minimize the combined power of the ionizer and neutralizer.

3. Design Analysis

3.1 Thrust Level Requirements

The density and velocity of the incoming gas is defined by the orbital altitude of the spacecraft. Given a spacecraft surface area, we can calculate the associated drag. We must now determine the optimum combination of ion flux and acceleration to provide thrust to balance the drag. The force balance can be expressed as

$$\frac{1}{2}\rho U^2 A_{\text{sat}} C_d = \rho U A_{\text{annulus}} \phi C_{\text{accel}}$$

Equation 3.1

ρ	density of the gas
U	orbital velocity of the satellite
A_{sat}	satellite's cross sectional area
C_d	coefficient of drag
Annulus	cross sectional area of annulus inlet
ϕ	ionization fraction
C_{accel}	increase in ion velocity after acceleration

The ionization fraction is driven by the electron cross section and current density. The increase in ion velocity after acceleration is driven by the electrostatic field strength. This velocity is also affected by the effectiveness of neutralizing the ions after acceleration. The ions can be neutralized by either combining with free electrons in the ambient plasma or by combining with electrons supplied by a neutralizer, similar to those used on traditional ion engines.

3.2 Ionization Cavity Design

3.2.1 General Considerations

The design should minimize power consumption for a given thrust requirement, yet maintain a size that is capable of being stowed for launch. The power drawn by the ionizing chamber can be varied by changing the electron current and voltage drop. These variables affect the fraction of neutrals that are ionized. As the fraction of neutrals ionized decreases, either the total mass flux through the ionization chamber must increase (i.e. increase inlet area) or the acceleration required per ion must increase for a given thrust level.

3.2.2 Magnetic Field Configuration

The magnetic field is aligned so the field lines are parallel to the axis of the annulus. This can be arranged by winding a solenoid around the outer annulus. The solenoid will create a nearly uniform magnetic field within the ionization cavity. The current that flows through the solenoid can be the same current as used by the ionizer filament itself.

The magnetic field is given by the current and the number, n , of windings per unit length of the ionization cavity,

$$B = \mu_0 i n$$

Equation 3.2

As the electrons travel from the cathode to the potential on the outer surface, they will experience a Lorentz force which will cause them to travel in a spiral path, circling the annulus. This configuration maximizes the path length traveled by the electrons before they reach the outer annulus. The large mean free path of the electrons necessitates such a configuration to increase the chances of an ionization before the electron reaches the outer annular surface.

3.2.3 Larmor Radius and Sizing

The path of an electron is curved as it travels through a magnetic field due to the Lorentz force, which is the cross product of the velocity and magnetic field. In a uniform magnetic field, the electron will travel in a circle due to conservation of angular momentum. The radius of this circle, called the Larmor radius, is given by

$$r_{\text{larmor}} = \frac{m_e v}{q_{\text{ion}} B}$$

Equation 3.3

The relationship between the Larmor radius and the thruster sizing determines the flux of ions. In traditional ion engines, the Larmor radius is very small compared to the length scale of the thruster. However, in this design, the Larmor radius is the same as the thruster's size.

3.2.4 Ionization Mechanics

NOTE: The material in this section is adapted from the course notes for MIT's Molecular Gas Dynamics of Space and Reentry class as developed by Prof. H. Wachman and Prof. D. Hastings.

3.2.4.1 The Collision Probability

Consider the stream of ambient gas as it enters the ionization section of the thruster's annulus. Ions are produced from collisions between electrons and neutrals. To determine the rate of collisions, let N_0 be the number of neutrals at time t_0 , and N the number of neutrals remaining at time t , without having been ionized between t_0 and t . Let Θ_c be that average number of ionizations per unit time that a neutral of the incoming stream suffers at time t (the average ionization rate per unit time at time t). Thus, Θ_c is the average ionization rate, or the average ionization frequency of a neutral moving at inlet velocity C .

The N neutrals that have not been ionized from t_0 to t will experience ionizations at a rate $N\Theta_c$ at time t , and will undergo $N\Theta_c dt$ ionizations between t and $t+dt$. Since an ionization removes a neutral from the group, the rate, dN/dt , at which neutrals are removed is equal to the rate at which they are ionized. Therefore,

$$-\frac{dN}{dt} = N\Theta_c$$

Equation 3.4

The number N of neutrals which remain in the selected group at time t , expressed as a function of Θ_c and time t , is

$$\int_{N_0}^N \frac{dN}{N} = \int_0^t -\Theta_c dt$$

Equation 3.5

thus,

$$N = N_0 e^{-\Theta_c t}$$

Equation 3.6

Θ_c is the fraction dN/N of a selected group that undergoes ionizations during some specified time interval dt . If the interval is made small enough so that within the time of an

experiment an ionization is observed during some intervals dt , and not observed during others, then Θ_c may be regarded as the probability of collision per unit time at speed C .

3.2.4.2 Free-Paths and Transit Times of the Surviving Neutrals

The time, t , is the total time measured from t_0 , through which the selected group is traveling through the ionizer, a time during which the group suffers $N_0 - N$ ionizations and its population is diminished by that many neutrals. Each of the N surviving neutrals traversed the same distance λ_f , ('free path') during t , and did so without ionization. Note the N surviving neutrals are still traveling at speed C . Thus, the free path, λ_f , is given by,

$$\lambda_f = Ct$$

Equation 3.7

allowing Equation 3.6 to be written

$$N = N_0 e^{-\Theta_c \frac{\lambda_f}{C}}$$

Equation 3.8

Since Θ_c represents the average ionization frequency at C , $1/\Theta_c$ is the mean time between ionizations for neutrals traveling at C so that

$$\Theta_c t = \frac{t}{t_c}$$

Equation 3.9

The time rate of change, $-dN/dt$, of the population of the original group, can now be expressed in terms of the actual time lapse from $t=0$ and the derivative of Equation 3.8,

$$-\frac{dN}{dt} = N_0 \Theta_c e^{-\Theta_c t}$$

Equation 3.10

Similarly, the number of ionizations per unit path-length can be expressed as

$$-\frac{dN}{d\lambda_f} = N_0 \frac{\Theta_c}{C} e^{-\Theta_c \frac{\lambda_f}{C}}$$

Equation 3.11

The number $|dN|$, of neutrals ionized between t and $t+dt$ is,

$$|dN| = N_o \Theta_c e^{-\Theta_c t} dt$$

Equation 3.12

while the number of neutrals that have free-paths lying between λ and $\lambda+d\lambda$ is

$$|dN| = N_o \frac{\Theta_c}{C} e^{-\Theta_c \frac{\lambda}{C}} d\lambda$$

Equation 3.13

3.2.4.3 The Mean Free Path and Probabilities

From the definition of Θ_c , the average distance between ionizations for neutrals moving at inlet speed C is C / Θ_c . This distance is defined as, λ_c , the mean free path at speed C . Thus the average distance a neutral travels before it is ionized is given by,

$$\lambda_c = \frac{C}{\Theta_c}$$

Equation 3.14

The ionization process can now be described in terms of probabilities associated with λ_c . Accordingly, we define $\phi(\lambda)$ as the probability that a neutral will travel at least a distance λ without collision. The number of neutrals that do so is N , hence $\phi(\lambda) = N/N_o$, so that for neutrals that travel at speed C , $\phi(\lambda)$ may be expressed as

$$\phi_\lambda = e^{-\frac{\lambda}{\lambda_c}}$$

Equation 3.15

With the substitution of Equation 3.14, this becomes

$$\phi_\lambda = e^{-\frac{\lambda \Theta_c}{C}}$$

Equation 3.16

The probability that a neutral will not be ionized as it travels through a distance equal to the mean free path is obtained by setting $\lambda = \lambda_c$ in Equation 3.16 which gives $\phi(\lambda_c) = 1/e = 0.37$. Shorter free paths have higher probabilities, and in the limit, the probability that a neutral will not be ionized through a distance $\lambda = 0$ is 1.

Every neutral will travel at least the distance $\lambda = 0$ without ionization, while only 37% of the neutrals may be expected to travel a distance λ_c without being ionized. Hence at $\lambda = \lambda_c$, $N = 0.37N_o$.

3.2.4.4 The Ionization Rate of a Constant Speed Electron Beam Moving Through a Gas of Neutrals

The ionization rate depends on the relative speeds and directions of the electrons and neutrals. This problem is simplified by considering the specific contributions of directions of motion and of speeds separately. For this reason, we consider the ionization rate for neutrals moving with velocity C_n into the electron gas in which all electrons are moving at the same speed C_e . Since the neutrals are entering axially and the electrons circulate radially, the velocity vectors are perpendicular. As a result, the magnitude of the relative velocity vector is

$$C_r = \sqrt{C_e^2 + C_n^2}$$

Equation 3.17

After defining the relative velocity vector, we can model the collision with a collision cylinder as depicted in Figure 3-1. The cross-section for ionization is given as the square of the combined radius, r_{12} , times π . The cross-section is also given in Figure 3-2. The volume of the collision cylinder is the product of the cross-section and the cylinder length. This length is given by the product of the relative velocity and time. Since the collision frequency is defined in terms of collisions per second, the collision frequency can be expressed as,

$$\Theta_C = N_n \sigma C_r$$

Equation 3.18

where N_n is the number density of neutrals and σ is the cross section for ionization.

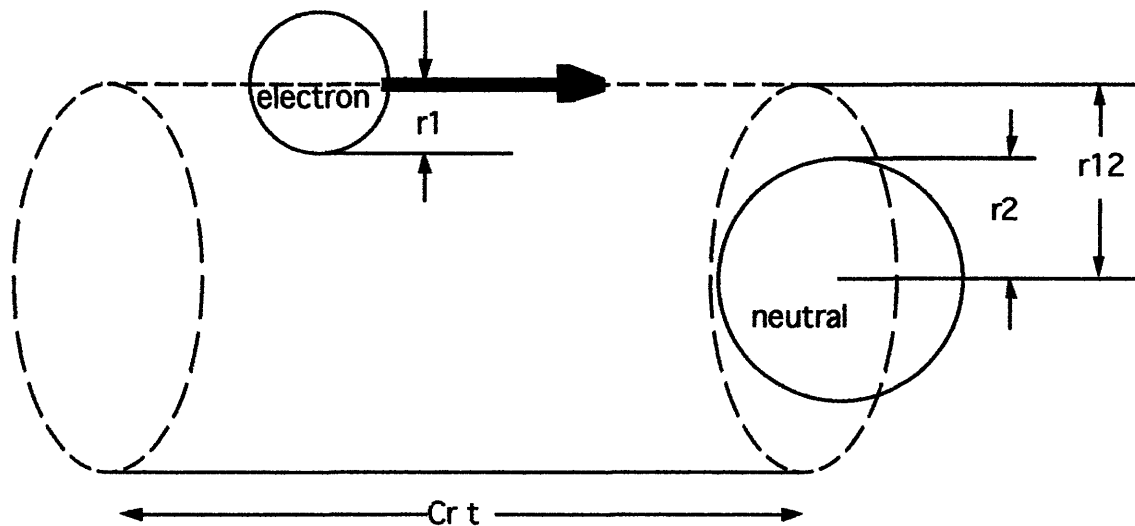


Figure 3-1² Collision Cylinder

3.2.4.5 Ionization Cross Section

The cross section for ionization of a neutral by an electron is a function of the electron's energy. It will be necessary to ionize the neutrals in the ambient gas before they can be accelerated to provide thrust. The relationship between ionization cross section and

² Sutton, George W. and Arthur Sherman, *Engineering Magnetohydrodynamics* McGraw-Hill 1965. p.82

electron energy is depicted in Figure 3-2. Although the maximum cross section values occur near 100 electron volts (eV), the actual ionization energy is only about 15 eV. When a neutral is ionized, the products are two lower energy electrons and an ion. The secondary electrons can produce further ionizations if their energy is increased.

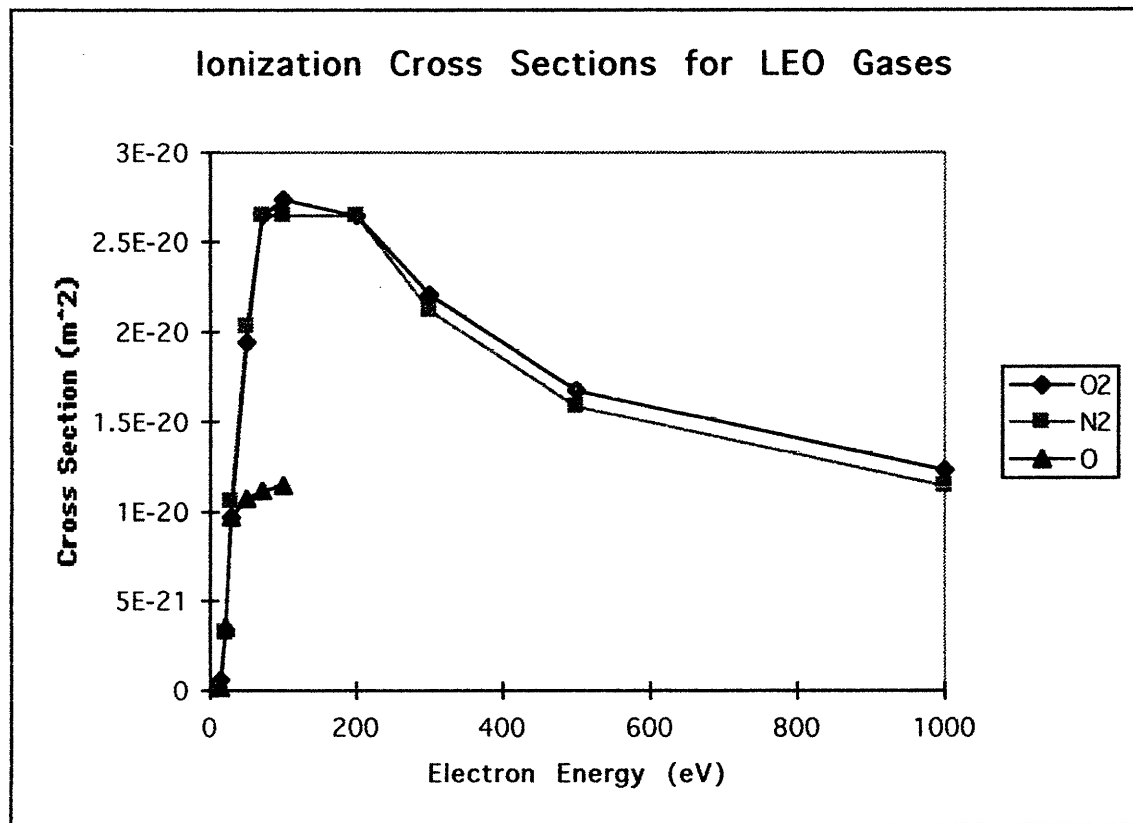


Figure 3-2³ Ionization Cross Section Versus Electron Energy

3.2.5 Space Charge Limitations in the Presence of a Magnetic Field

The density of the electron swarm circling the annulus is limited by the electric field strength. When the charge density causes the electric field at the emitter to become zero, no more charge can be drawn from the electron emitting filament.

The motion of the electrons is governed by both the electric and magnetic fields. Motion due to the electric potential field, Φ , is given by,

$$q \Phi = \frac{m v^2}{2}$$

Equation 3.19

³ McDowell, M.R.C. *Atomic Collision Processes* The Proceedings of the Third International Conference on the Physics of Electronic and Atomic Collisions. University College, London, 22nd-26th July, 1963. North-Holland Publishing Company-Amsterdam.

The motion due to the magnetic field is given by Equation 3.3 which defines the Larmor radius. These equations can be combined to eliminate the velocity variable,

$$\Phi = \frac{q B^2 r^2}{2 m_e}$$

Equation 3.20

This potential field must satisfy Poisson's equation. For the annulus, this can be expressed in polar coordinates as

$$\frac{d^2\Phi}{dr^2} + \frac{1}{r} \frac{d\Phi}{dr} = \frac{q N_e}{\epsilon_0}$$

Equation 3.21

substitution of the expression for the potential into Poisson's equation gives an expression for the number density of electrons, N_e ,

$$N_e = \frac{2 B^2 \epsilon_0}{m_e}$$

Equation 3.22

This solution demonstrates that the electron density in the annulus is only a function of the magnetic field. However, the geometry of the thruster and the magnetic field strength specify the necessary voltage for this condition to exist, according to Equation 3.20.

3.2.6 Ion Mass Flux

The mechanics of ionization can be combined with the cavity geometry and gas properties to determine the flux of ions which can be created from an incoming stream of neutrals.

3.2.6.1 Ionization Frequency in the Magnetic Field

The ionization frequency is given by Equation 3.18. Since the electrons will be at energies on the order of hundreds of electron volts, their velocities will be significantly greater than the velocity of the incoming neutral stream. This allows us to simplify the expression for ionization frequency to,

$$\Theta_c = N_e v_e \sigma$$

Equation 3.23

From Figure 3-2 we see a resonance in cross section energy near 100 eV. At energies above 100 eV, the cross section fall in the range of about 10^{-20} m². The number density is given by Equation 3.22 and the velocity is given by Equation 3.3. These expressions can be combined to express the ionization frequency in terms of the magnetic field and thruster geometry,

$$\Theta_c = \frac{2\varepsilon_0 q \sigma B^3 r}{m_e^2}$$

Equation 3.24

The relationship between thruster size, magnetic field strength, and ionization rate is graphically displayed in Figure 3-3.

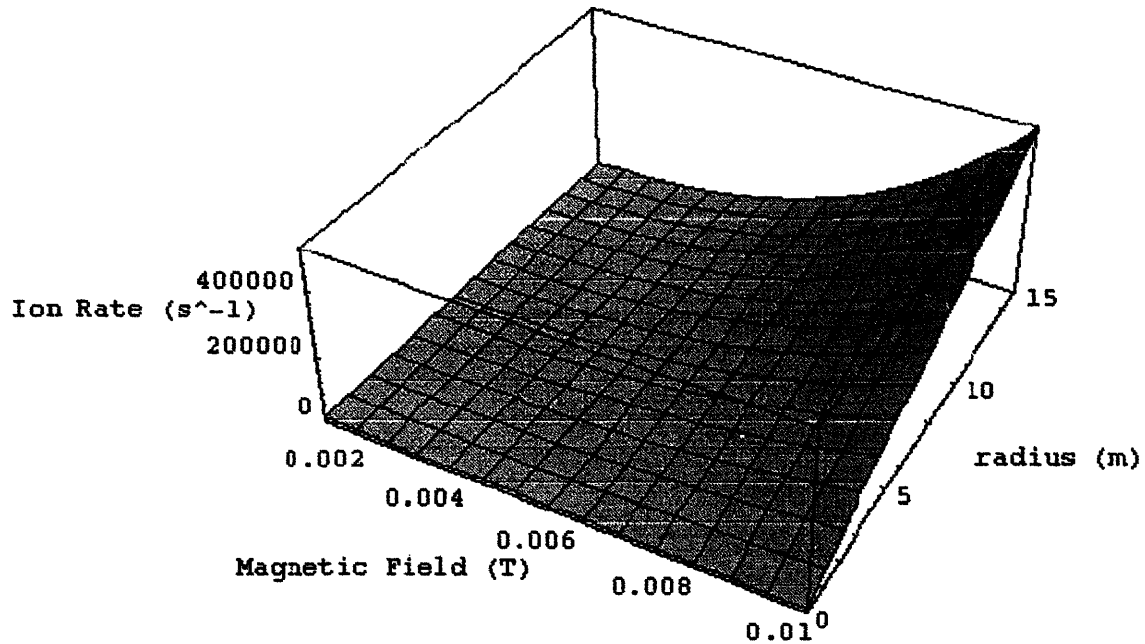


Figure 3-3 Ionization Rate Versus Radius and Magnetic Field

3.2.6.2 Ionization Fraction and Mass Flux

Equation 3.16 gives the fraction of neutrals which survive without ionization after traveling a certain length. This equation can be manipulated to find fraction of neutrals in a stream that are ionized. More specifically, we can also include the expression for ionization rate found in Equation 3.24 to determine the ionization fraction of a neutral stream after traveling a distance λ ,

$$\phi_{\text{ionized}} = 1 - e\left(-\lambda \frac{2\epsilon_0 q \sigma B^3 r}{m_e^2 C_n}\right)$$

Equation 3.25

The ionization fraction as a function of magnetic field and radius is displayed in Figure 3-4.

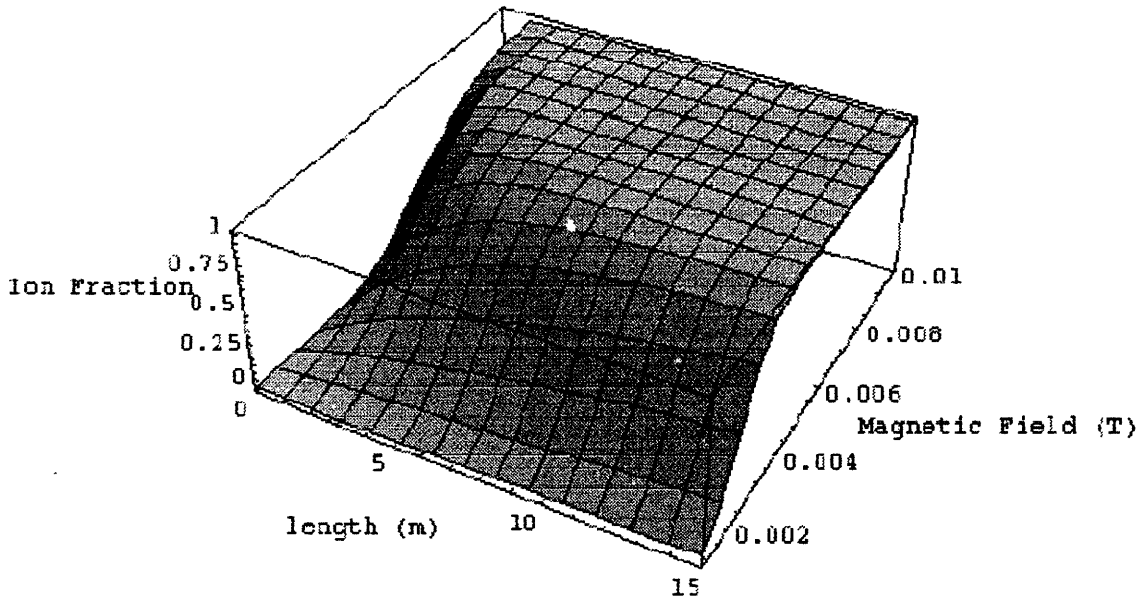


Figure 3-4 Ionization Fraction Versus Length and Magnetic Field

The integration of Equation 3.25 around the annulus determines the total ion mass flux that exits the ionization cavity,

$$\text{Flux} = \int_0^{r_0} N_n \phi_{\text{ionized}} v_n 2 \pi r dr$$

Equation 3.26

The ion flux as a function of length and radius is displayed in Figure 3-5.

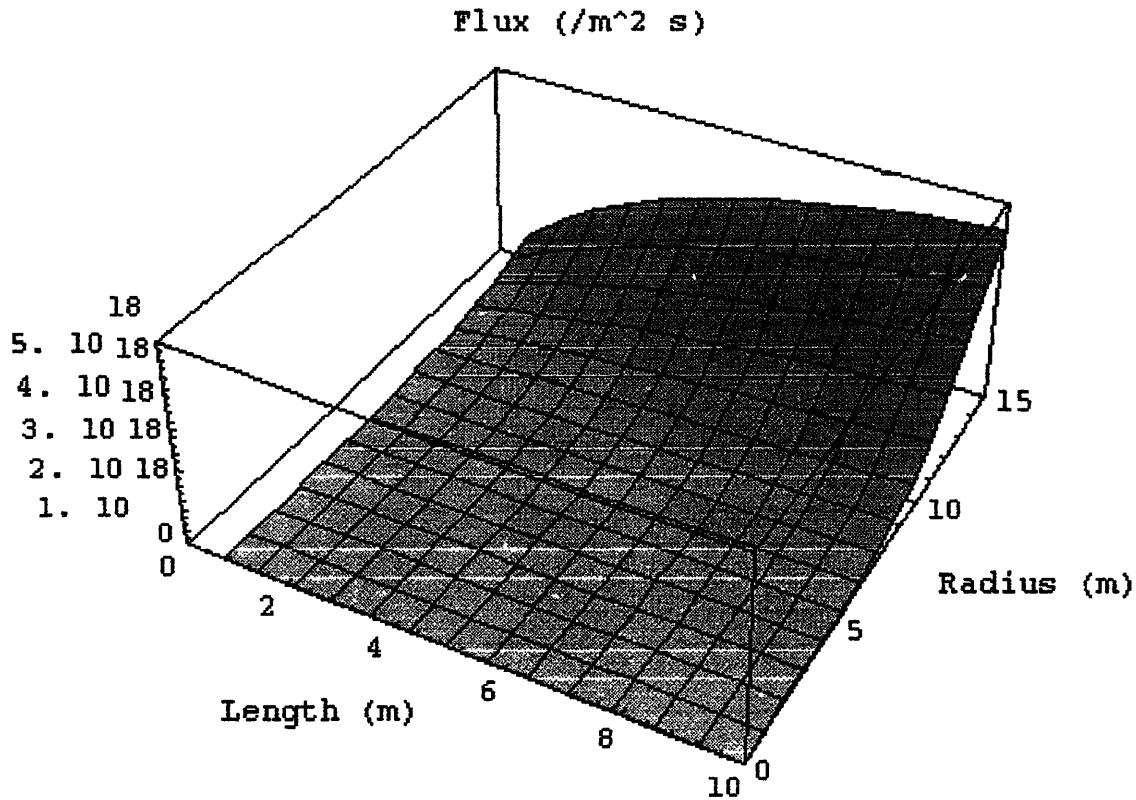


Figure 3-5 Flux Versus Geometry

3.3 Configuration of the Accelerator

The electrostatic accelerator will resemble the accelerator in a Kaufman engine in several ways. It will consist of two closely spaced metal grids which carry a high potential voltage. It faces the same space charge limitations on current density. However, it differs in that its open fraction to neutrals is maximized. In fact, the grid will more resemble a sparse wire mesh. This is because we do not want to impede the passage of neutrals through the thruster. With these motivations, the accelerator grid will minimize material that may impede the passage of the ions and neutrals.

3.3.1 Space Charge Limited Current

The electrostatic field used to accelerate the ions approaches a lower limit as it is just neutralized at the source plane by the distributed intervening charge. This is called space charge limited current⁴. Unlike traditional ion accelerators, the thruster accelerates ions which are already moving at a high velocity. This boundary condition requires a unique solution for the space charge limitation of the accelerating grid.

⁴ Jahn, Robert G. *Physics of Electric Propulsion* McGraw-Hill Series in Missile and Space Technology. 1968.

3.3.1.1 Poisson's Equation

The acceleration cavity can be modeled as a one dimensional flow of charge between two infinite plates with a potential voltage. This arrangement can be described by Poisson's equation,

$$\frac{d^2V}{dx^2} = -\frac{\rho}{\epsilon_0}$$

Equation 3.27

and the following definitions of charge density and current

$$\rho = nq$$

Equation 3.28

$$i = nqv$$

Equation 3.29

where the velocity, v , of the ion is given by conservation of energy,

$$v = \sqrt{\frac{2q(V_0 - V)}{m} + v_{initial}^2}$$

Equation 3.30

with $v_{initial}$ being the initial velocity of the ion as it enters the acceleration grid. Since we assume the momentum of the ionizing electron to be small compared to the momentum of the neutral, the initial velocity of the ion is assumed to be equal to the inlet velocity.

The solution of Poisson's Equation can be further assisted by the following identity,

$$\frac{d^2V}{dx^2} = \frac{1}{2} \frac{d}{dV} \left(\frac{dV}{dx} \right)^2$$

Equation 3.31

Combining these equations give,

$$\frac{1}{2} \frac{d}{dV} \left(\frac{dV}{dx} \right)^2 = - \frac{i}{\epsilon_0 \sqrt{\frac{2q(V_0 - V)}{m} + v_{initial}^2}}$$

Equation 3.32

which upon integration is

$$\left(\frac{dV}{dx}\right)^2 = \frac{2 i m}{\epsilon_0 q} \sqrt{\frac{2q(V_o - V)}{m} + v_{initial}^2} + C$$

Equation 3.33

The gradient of the potential is the electric field. This equation can now be solved by appropriate substitution of the electric field boundary conditions.

3.3.1.2 The Electric Field with an Ion Current Entering the Grid

To find the value of the constant in Equation 3.33 we must determine the electric field, dV/dx , at the entrance to the grid. The electric field must be continuous across the first accelerator grid according to Poisson's Equation. Therefore, determination of the electric field on one side of the grid defines the electric field on the other. Consider a hypothetical space charge limited accelerator where the ions have zero initial velocity and are accelerated to a velocity equal to v_{exit} . If we can find the electric field at the exit of this arrangement, we will know the electric field at the entrance of our accelerator by setting $v_{exit} = v_{initial}$.

To solve for the electric field of the hypothetical accelerator, let $v_{initial} = 0$ in Equation 3.33 and apply the boundary condition at the inlet that the voltage is V_o and the electric field is 0. This gives the result that $C=0$. Next, consider the electric field at the exit of the accelerator where the voltage is 0,

$$\frac{dV}{dx} = \sqrt{\frac{2 i}{\epsilon_0}} \sqrt{\frac{2mV_o}{q}}$$

Equation 3.34

V_o in Equation 3.34 is the voltage required to accelerate a charge, q , of mass, m , to the velocity $v_{initial}$ according to Equation 3.30. The current is also given by Equation 3.29 with $v=v_{initial}$. With these substitutions, the electric field is given by

$$\frac{dV}{dx}_{exit} = v_{initial} \sqrt{\frac{2Nm}{\epsilon_0}}$$

Equation 3.35

Now that we know the electric field of the ion beam as it exits the hypothetical accelerator, we also know the electric field at the entrance of the actual acceleration grid. The constant, C , in Equation 3.33 is 0 from substitution the expression for the electric field given in Equation 3.35 and evaluating at the entrance of the accelerator where the voltage is V_o .

3.3.1.3 Integration of Poisson's Equation

After substituting for $C=0$, we can separate variables to solve Poisson's Equation,

$$\left(\sqrt{\frac{2q(V_o - V)}{m} + v_{initial}^2}\right)^{-1} dV = \sqrt{\frac{2 i m}{\epsilon_0 q}} dx$$

Equation 3.36

and make the change of variables

and make the change of variables

$$z = \sqrt{\frac{2q(V_o - V)}{m} + v_{initial}^2}$$

Equation 3.37

$$dz = -\frac{q}{m} \left(\frac{2q(V_o - V)}{m} + v_{initial}^2 \right)^{-\frac{1}{2}} dV$$

Equation 3.38

so we can substitute for dV according to

$$dV = -\frac{m}{q} z dz$$

Equation 3.39

resulting in the simplified differential equation,

$$-\frac{m}{q} \sqrt{z} dz = \sqrt{\frac{2im}{\epsilon_o q}} dx$$

Equation 3.40

This can be easily integrated to give

$$-\frac{2m}{3q} z^{\frac{3}{2}} = \sqrt{\frac{2im}{\epsilon_o q}} x + C$$

Equation 3.41

Note that at $x=0$, $V=V_o$, so $z=v_{initial}^2$ which requires

$$-\frac{2m}{3q} v_{initial}^{\frac{3}{2}} = C$$

Equation 3.42

Substituting for z and applying the boundary condition at end of the grid of $V=0$ at $x=x_a$ to give the space charge limited current,

$$i = \frac{2\epsilon_o m}{9q} \left(\frac{v_{initial}^{\frac{3}{2}} - \left(\frac{2qV_o}{m} + v_{initial}^2 \right)^{\frac{3}{4}}}{x_a} \right)^2$$

Equation 3.43

note that for $v_{initial}=0$, Equation 3.43 reduces to its familiar form of,

$$i = \frac{4\epsilon_0}{9} \sqrt{\frac{2q}{m}} \frac{V_o^{3/2}}{x_a^2}$$

Equation 3.44

where the variables are

i	current
ϵ_0	permittivity of free space
q	charge of ion
m	mass of ion
V_o	voltage potential
x_a	gap between grids

3.3.1.4 Practical LEO Space Charge Limited Current Value

In an ion accelerator, the highest practical limit of the electric field is about 10^7 Volts/meter. This limitation places a boundary on the minimum gap spacing, x_a , for a given voltage, according to⁵

$$E_a = \frac{4V_o}{3x_a}$$

Equation 3.45

Due to the manufacturing limitations, the minimum gap spacing is limited to about 0.005 meters. This corresponds to a voltage of 37500 volts. We can now calculate a space charge limited current in the LEO environment at an orbit of 200 Km with the following values:

$$\epsilon_0 = 8.85418781761 \cdot 10^{-12}$$

$$q = 1.602117733 \cdot 10^{-19} \text{ C}$$

$$m_{ion} = 19.79 \text{ g/mol} / (6.0221367 \cdot 10^{23} \text{ atoms/mol}) / 1000 \text{ g/Kg}$$

$$\text{Practical LEO Space Charge Limited Current} = 0.1515 \text{ Amps/m}^2$$

The ion flux from the ionizer must not exceed the practical LEO space charge limited current.

3.4 Design Optimization

The relationships between ionization chamber geometry, magnetic field, and voltage can be combined to determine the optimum configuration to minimize ionizer power. However, a minimum power ionizer may result in a sub-optimal power for the accelerator. For example, the ionizer power decreases as ion mass flux decreases. However, the thrust requirement is fixed because the drag is determined by the fixed area of the spacecraft. As a result, the accelerator must give a smaller mass flux a greater velocity to maintain the same thrust level. Since accelerator power increases as the square of velocity, the accelerator power requirement may rise faster than the ionizer power falls.

From the graphs, it appears that there is no constraint on increasing the size of the thruster to improve performance. As systems trade between thruster mass and power

⁵ Jahn, p. 146.

requirement must be made. A larger thruster will have a greater mass, but require less power. This trade must be made in the context of the entire spacecraft systems design.

To gain a feel for the physical dimensions and properties of the design, we will consider a specific thruster that will balance the drag on a spacecraft at 200 Km which has a surface area of 1 m². The dimensions of the thruster should be within an order of magnitude of the satellite dimensions. Within these constraints, the minimum power required for this mission may be determined.

3.4.1 Ionizer Power

The ionizer power arises from the ionization process. When an electron strikes a neutral, it will fall from its orbit around the annulus and strike the anode. As these electrons cross the potential, their current will draw power. Since the number of ionizations is equal to the number of electrons conducted to the anode, the electron flux is equal to the ion flux. Therefore, the ionizer power is the product of the ion flux and the ionizer voltage,

$$\text{Ionizer Power} = (\text{Flux}) q V_{\text{ionizer}}$$

Equation 3.46

3.4.2 Jet Power

The ions ejected from the accelerator must be neutralized to maintain charge neutrality and allow the ions to escape the potential of the accelerator. The electrons which are emitted to neutralize the ions must be supplied at a voltage equal to the acceleration voltage. Since the ion flux will equal the electron flux, the power drawn by the neutralizer is equal to the jet power. Thus, the power consumed by the accelerator can be expressed as,

$$\text{Jet Power} = (\text{Flux}) q V_{\text{accelerator}}$$

Equation 3.47

3.4.3 Total Power

As discussed earlier, minimization of one power source may not necessarily minimize the total thruster power requirements. As the thruster power is minimized, the combination of the ionizer and jet power must be considered.

$$\text{Total Power} = (\text{Flux}) q (V_{\text{accelerator}} + V_{\text{ionizer}})$$

Equation 3.48

3.4.4 Thrust Requirements

The drag per unit area of spacecraft is given by

$$\frac{\text{Drag}}{A_{\text{sat}}} = \frac{1}{2} N_n m_n v_n^2 C_d$$

Equation 3.49

At 200 Km, the drag of a spacecraft with an area of 1 m² is 0.021 N. This fixed constraint can be set equal to the expression for thrust,

$$\text{Thrust} = \text{flux } m_{\text{ion}} \sqrt{\frac{2 q V_{\text{accel}}}{m_{\text{ion}}}} = 0.021 \text{ N}$$

Equation 3.50

3.4.5 Optimization of Physical Dimensions for Minimum Power

The constraint of Equation 3.50 allows the elimination of the acceleration voltage from Equation 3.48. The total power can now be minimized with respect to the ionizer voltage. This minimum power is a function of thruster's length and radius. The minimum power as a function of these physical dimensions is displayed in Figure 3-6 and rescaled in Figure 3-7.

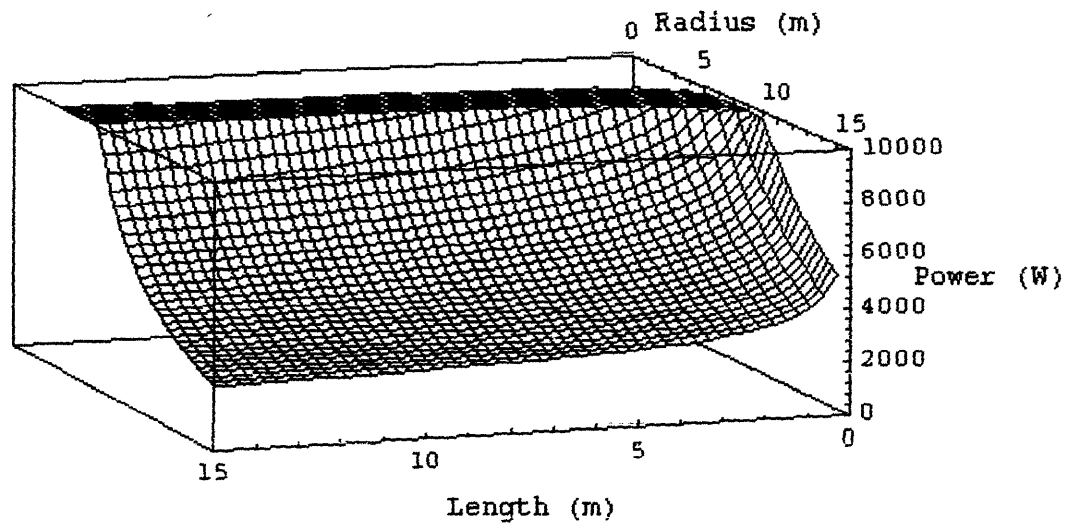


Figure 3-6 Power Versus Geometry

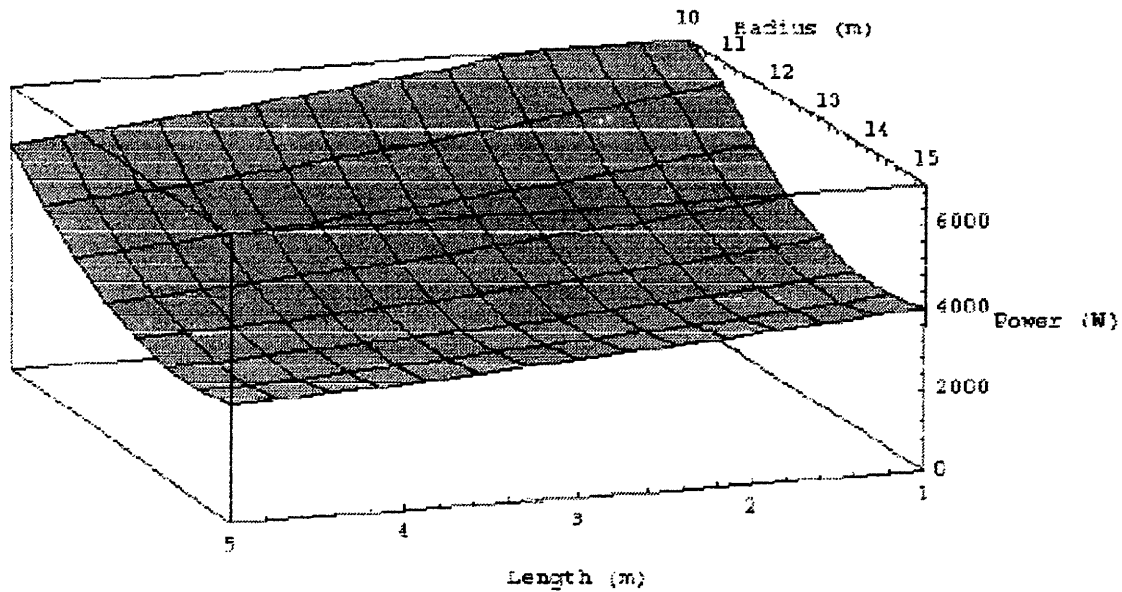


Figure 3-7 Power Versus Geometry (Local View)

3.4.6 Example Values

From Figure 3-7 we can select a length and radius to define the thruster configuration. This selection will determine the mass of the thruster. As a result, any design decisions must be made in the context of the complete spacecraft system design. However, we can select a thruster which has an ionization chamber length of 5 m and a radius of 15m to illustrate the corresponding thruster parameters,

Parameter	Value
Radius	15 meters
Length	5 meters
Accelerator Voltage	3796 Volts
Ionizer Voltage	1610 Volts
Power	2877 Watts
Thrust	0.021 Newtons
Magnetic Flux	0.002 Tesla
Solenoid Windings (from Equation 3.2)	15000
Accelerator Grid Spacing (charge limit)	0.64 meters
Solar Panel Size (at 210 Watts/m ²)	13.7 sq. meters

4. Conclusions and Recommendations

4.1 Applicability of Ion Propulsion to LEO Satellites

The utilization of ambient gas as a propellant for LEO ion propulsion to negate the effects of drag is limited to orbital altitudes near 200 Km. At higher altitudes, the propellant requirements are low enough to enable use of existing technology. At lower altitudes, the power requirements become prohibitively large.

The thruster design for low power requires large dimensions compared to the spacecraft. The power is most sensitive to the radius of the thruster, because it is directly coupled to the mass flow being accelerated. The marginal benefit from increasing the length of the thruster is small, since almost complete ionization is achieved after only a few meters. The solar panel area required to power the thruster is about ten percent of the total thruster area. The large size of the thruster could result in a significant mass. The size also complicates stowage and deployment. The magnetic field of the ionizer can be created by a solenoid that uses the current powering the thruster.

4.2 Suggestions for Further Analysis

A constant value for the ionization cross section was used. With a numerical model of the electron velocities, the ionization cross section could be applied as a function of energy. This model could also account for the motion of secondary electrons after a collision which may result in further ionizations--reducing ionizer power requirements.

This analysis also decouples the electric field of the ionizer cavity from the accelerator grids. If the systems design requires these components to be close together, an analysis to the electric field interactions must be done to account for perturbations in the electron density distribution and space charge limitations.

The modeling of the thruster assumed the drag on the accelerator grid mesh to be negligible and included with the fixed area of the spacecraft. However, the mesh will contribute to the drag and this drag will increase with the size of the mesh. The power increases due to excess drag will constrain on the radius size for minimum power. To perform this analysis, a detailed design of the accelerator grid must be performed to determine its contribution to drag.

The drag was assumed constant and set equal to the thrust. This assumed the number density to be constant with time and that the thruster operated continuously. However, the number density varies daily and seasonally. Furthermore, the 90 minute orbit at 200 Km requires the satellite to be in darkness over half of its operational time. For the thruster to operate continuously, batteries will be required. The alternative of intermittent operation may introduce eccentricity into the orbit. The variations in neutral density and thruster operation should be included in the early stages of a systems design process.

The thruster is large and diaphanous, presenting a great challenge to the mechanical designer. The structure must not only be rigid in operation, but stowable for launch. The mechanism for deployment must be reliable and maintain the integrity of the design. Finally, this design must maintain a very low mass to present any benefit over carrying onboard propellant.

4.3 Suggestions for Design Improvements

The electron swarm could be replaced by a plasma. If a cloud of slow ions could be contained in the ionization cavity with the circulating electrons, the electron number density could be increased beyond the original space charge limitations. The increased electron density would enable a smaller, more efficient thruster. The thruster may also need electromagnetic shielding depending upon the communications mission of the spacecraft and the noise introduced from the thruster.

Capturing the slow neutrals after they collide with the spacecraft will increase the ionization fraction. A design which collects these slow neutrals will be smaller and require less ionization power.

Acknowledgment

The author would like to thank the Massachusetts Space Grant Consortium for sponsoring his graduate studies through the award of the NASA Space Grant Fellowship.

5. Appendix

The following code was used with the *Mathematica* software package :

```
epso=8.85418781761 10^-12
ionmass=3.28620902943 10^-26
charge=1.60217733 10^-19
electronmass=9.1093897 10^-31
crossection=10^-20
Ne[B_]=2 B^2 epso / electronmass
v[r_,B_]=charge r B /electronmass
thetaC2[r_,B_]=v[r,B] Ne[B] crossection
Plot3D[thetaC2[r,B],{B,10^-3,10^-2},{r,0,15},
  AxesLabel->{"Magnetic Field (T)", "radius (m)", "Ion Rate (s^-1)"}]

phi2[lambda_,neutralspeed_,r_,B_]=1-Exp[-lambda thetaC2[r,B]/neutralspeed]
Plot3D[phi2[1,8000,1,B],{1,0,15},{B,10^-3,10^-2},AxesLabel->{"length (m)",
  "Magnetic Field (T)", "Ion Fraction"}]

B[r_,V_]=r (2 electronmass V/charge)^(1/2)
flux3[lambda_,neutralspeed_,ri_,ro_,V_,Nn_]=Nn Integrate[phi2[lambda,
  neutralspeed,r,B[r,V]] 2 Pi r,{r,ri,ro}]

Plot3D[flux3[5,8000,ri,ro,2877,10^16],{ri,.1,15},{ro,.1,15},PlotRange->
  {0,4 10^18},AxesLabel->{"Inner Radius (m)", "Outer Radius (m)",
  "Flux (m^-3)"}]

thrust3[lambda_,neutralspeed_,ri_,ro_,Vionizer_,Nn_,Vaccel_]=flux3[lambda,
  neutralspeed,ri,ro,Vionizer,Nn] ionmass (2 charge Vaccel/ionmass)^(1/2)

Solve[thrust3[lambda,neutralspeed,ri,ro,Vi,Nn,Va]-.021==0,Va]
Assign result of this calculation to Va[lambda_,neutralspeed_,ri_,ro_,Vi_,Nn_]
jetpower[lambda_,neutralspeed_,ri_,ro_,Vionizer_,Nn_,Vaccel_]=thrust3[lambda,
  neutralspeed,ri,ro,Vionizer,Nn,Vaccel] (2 charge Vaccel/ionmass)^(1/2) /2

totalpower[lambda_,neutralspeed_,ri_,ro_,Vionizer_,Nn_,Vaccel_]=
  jetpower[lambda,neutralspeed,ri,ro,Vionizer,Nn,Vaccel]+ionpower[lambda,
  neutralspeed,ri,ro,Vionizer,Nn]

fixedpower[lambda_,neutralspeed_,ri_,ro_,Vionizer_,Nn_]=totalpower[lambda,
  neutralspeed,ri,ro,Vionizer,Nn,Va[lambda,neutralspeed,ri,ro,Vionizer,Nn]]

Plot3D[FindMinimum[Evaluate[fixedpower[1,8000,0,r,Vionizer,10^16]],
  {Vionizer,5000,100,100000}],{1,0,5},{r,10,15}]

FindMinimum[Evaluate[fixedpower[5,8000,0,15,Vionizer,10^16]],{Vionizer,
```

```

5000,100,500000}]

N[Va[5,8000,0,15,1610.45,10^16]]
N[totalpower[5,8000,0,15, 1610.45,10^16,1984.69]]
N[thrust3[5,8000,0,15, 1610.45,10^16,1984.69]]
N[flux3[5,8000,0,15, 1610.45,10^16]]
N[B[15,2877.17]]
j[Vo_,vi_,xa_]=2 eps0 ionmass /(9 charge xa^2) (vi^(3/2) - (2 charge Vo/ionmass +
vi^2)^(3/4) )^2

N[j[3796.22,8000,.,64]]
N[flux3[5,8000,0,15, 1610.45,10^16] charge/(Pi 5^2)]
Plot3D[FindMinimum[Evaluate[fixedpower[1,8000,0,r,Vionizer,10^16]],{Vionizer,
5000,100,100000}],{1,0,15},{r,0,15},PlotPoints->50]

mingraf=%
Show[mingraf,ViewPoint->{10,30,5},PlotRange->{{0,15},{0,15},{0,10000}},
AxesLabel->{"Length (m)","Radius (m)","Power (W)"}]

```